Direct Imaging of Conducting and Insulating Submolecularly Wide Pathways in an Organic Semiconductor

Andrew J. Lovinger,* Howard E. Katz, and Ananth Dodabalapur

Bell Laboratories, Lucent Technologies, Murray Hill, New Jersey 07974

Received June 4, 1998
Revised Manuscript Received September 2, 1998

The recent intense quest for development of printed, flexible, plastic-based flat-panel displays and other electronic circuits requires electroactive organic or polymeric semiconductors capable of being fabricated into thin-film transistors (TFTs). Creation of such TFTs has now been demonstrated with a number of organic materials, beginning with the pioneering work of Garnier et al.,[1,2] including oligothiophenes,[3−5] substituted naphthalenes,[6] phthalocyanines,[7] pentacene,[8−10] and others,[11−13] and have yielded devices with mobilities in the range of amorphous silicon. Their conduction mechanism involves charge transport across $\pi-\pi$-stacks of molecules. All of these classes of organic semiconductors that exhibit high mobilities have been found to adopt a highly ordered preferred orientation of molecules essentially normal to the substrate to maximize the flow of charges from source to drain electrodes. Here, we demonstrate a new morphology consisting of a three-dimensional percolation-type network. We also image for the first time the *submolecular* regions of an organic semiconductor (α,*ω*-dihexyl-α-hexathiophene) that self-align to create conducting and insulating channels. In this sense, we visualize the supramolecular pathways through which the electronic charges flow in this organic semiconducting material.

The experiments were carried out on α,*ω*-dihexyl-α-hexathiophene (DHα6T),[14] which is among the more promising TFT materials: its mobility (5×10^{-2} cm^2/Vs) is slightly higher than that of the prototypical organic semiconductor (α-hexathiophene or α6T) and, contrary to most organic transistor materials, it is solution-processable in low-boiling solvents (e.g., xylene),[4] thus bringing us closer to the realization of printed transistor technology. DHα6T was synthesized and purified as we described before,[4,5] i.e., through the monohexyl trimer via a polar substituted intermediate. Thin films were deposited by vacuum evaporation onto substrates nominally at room temperature. The semiconductor was simultaneously sublimed onto both Si/SiO_2 wafers for electrical determination of its transistor characteristics using the typical "bottom contact" electrode geometry[15] and carbon-coated copper grids for structural and morphological analysis by high-resolution transmission electron microscopy (TEM).[16] The former yielded mobilities in the same range as obtained previously,[4,5,15] i.e., 0.03−0.05 cm^2/Vs. The latter were obliquely shadowed with Pt/C and examined under bright-field TEM and electron diffraction.

Among the morphologies obtained, a highly interesting one is seen in Figure 1a to consist of an interlaced network of crystals that exhibit a wide range of electron contrast as they randomly and gradually change orientations on the substrate. This morphology is very different from the common ones seen in evaporated semiconducting organics: the typical morphology of the parent semiconductor, α6T, shown for comparison in the inset to Figure 1b, consists of very small (ca. 20 nm) irregular grains;[16,17] as a result of this small size, the grain boundaries play a dominant role in restricting charge transport. On the contrary, the morphology in Figure 1a shows much longer and well interconnected crystals, for which the role of grain boundaries is therefore minimized. This gradually curved and undulating DHα6T morphology also implies departures from the preferred nearly end-on substrate orientation found to date for the molecules of all high-mobility vacuum-sublimed organic-transistor materials,[6,8−11,13−17] including in fact the majority of DHα6T;[14,15,18] we are as yet uncertain of the reasons for this unusual morphology.[18] Specifically, as evidenced by our electron-diffraction results (insets within Figure 1a), the reflections at 0.457, 0.392, and 0.321 nm arise from the side-by-side packing of molecules essentially perpendicular to the substrate, whereas the major reflection next to the beam stop (at 3.52 nm) represents the spacing of the molecular layers and therefore originates from DHα6T chains that are nearly *parallel* to the substrate.

The location of these latter chains is identified under low-dose electron irradiation, which allows preservation

(1) Fichou, D.; Horowitz, G.; Nishikitani, Y.; Roncali, J.; Garnier, F. *Synth. Met.* **1989**, *28*, C729.
(2) Horowitz, G.; Fichou, D.; Peng, X. Z.; Garnier, F. *Synth. Met.* **1991**, *41*, 1127.
(3) Akimichi, H.; Waragai, K.; Hotta, S.; Kano, H.; Sakaki, H. *Appl. Phys. Lett.* **1991**, *58*, 1500.
(4) Katz, H. E.; Torsi, L.; Dodabalapur, A. *Chem. Mater.* **1995**, *7*, 2235.
(5) Katz, H. E.; Dodabalapur, A.; Torsi, L.; Elder, D. *Chem. Mater.* **1995**, *7*, 2238.
(6) Bao, Z.; Lovinger, A. J.; Brown, J. *J. Am. Chem. Soc.* **1998**, *120*, 207.
(7) Bao, Z.; Lovinger, A. J.; Dodabalapur, A. *Appl. Phys. Lett.* **1996**, *69*, 3066.
(8) Laquindanum, J. G.; Lovinger, A. J.; Dodabalapur, A.; Katz, H. E. *Chem. Mater.* **1996**, *8*, 2542.
(9) Gundlach, D. J.; Lin, Y. Y.; Jackson, T. N. *IEEE Electron. Device* **1997**, *18*, 87.
(10) Dimitrakopoulos, C. D.; Brown, A. R.; Pomp, A. J. *J. Appl. Phys.* **1996**, *80*, 2501.
(11) Tsumura, A.; Koezuka,; Ando, T. *Appl. Phys. Lett.* **1986**, *49*, 1210.
(12) Bao, Z.; Lovinger, A. J.; Dodabalapur, A. *Appl. Phys. Lett.* **1996**, *69*, 4108.
(13) Laquindanum, J. G.; Katz, H. E.; Lovinger, A. J. *J. Am. Chem. Soc.* **1998**, *120*, 664.
(14) Garnier, F.; Yassar, A.; Hajlaoui, R.; Horowitz, G.; Deloffre, F.; Servet, B.; Ries, S.; Alnot, P. *J. Am. Chem. Soc.* **1993**, *115*, 8716.
(15) Katz, H. E.; Laquindanum, J. G.; Lovinger, A. J. *Chem. Mater.* **1998**, *10*, 633.
(16) Lovinger, A. J.; Davis, D. D.; Dodabalapur, A.; Katz, H. E. *Chem. Mater.* **1996**, *8*, 2836.
(17) Lovinger, A. J.; Davis, D. D.; Dodabalapur, A.; Katz, H. E.; Torsi, L. *Macromolecules* **1996**, *29*, 4952.
(18) The different morphologies obtained for DHα6T in different studies may reflect highly sensitive dependence of crystal nucleation, growth, and orientation on details of the deposition process, e.g. subtle variations in deposition rate, source temperature, source-to-substrate distance, and vacuum.

10.1021/cm980402u CCC: $15.00
Published on Web 10/22/1998

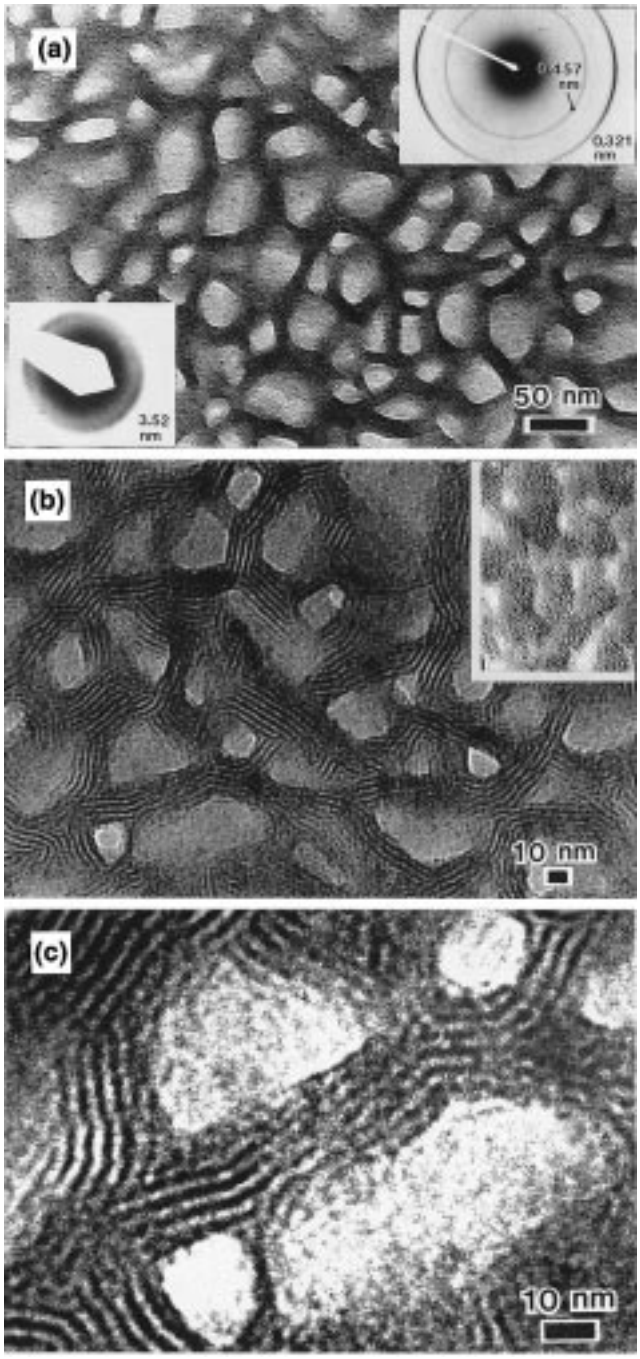

Figure 1. (a) Bright-field transmission electron micrograph of DHα6T, showing a network morphology of interconnected crystals with random orientations. The electron-diffraction pattern at the upper right consists of reflections arising from the side-by-side packing of the molecules. The diffraction pattern at the lower left is a magnification of the central region around the beam stop, demonstrating the presence of a reflection at 3.52 nm which arises from the end-to-end spacing of molecules essentially parallel to the film. (b) Low-dose electron micrograph at higher magnification, revealing the presence of lattice fringes parallel to the growth direction of those crystals that are oriented edge-on to the substrate. For comparison, the typical morphology of organic semiconductors that consists of very small, irregular grains is shown at the same maginification in the inset for the parent semiconductor, α6T. (c) At even higher magnification, these lattice fringes in DHα6T are seen to have a periodicity of 3.6 nm, consistent with the thickness of end-to-end molecular layers, and to extend in close contact across crystal boundaries over lengths of many tens of nanometers.

of diffraction contrast during photographic exposure and has been used successfully to elucidate the lattice structure and defects of other organic materials.[19−21] As seen in Figure 1b, this results in visualization of lattice fringes having a measured periodicity of 3.6 nm. Importantly, these fringes are observed *only within the dark rodlike crystals* and run along their lengths. This confirms the edge-on orientation of those crystals and shows that they consist on average of 5−6 molecular layers that have crystallographic continuity over many tens of nanometers. Between these edge-on crystals are others in different orientations, which therefore do not exhibit fringes because they are not in the diffracting condition. Very significantly in terms of charge-carrier mobility, the contact and continuity of the lattice fringes extends beyond crystal boundaries: at the higher magnification of Figure 1c a variety of edge dislocations and other defects are observed, yet many of the dark fringes are seen to match and be coupled effectively among different crystals. This establishes a percolation-type network of crystallographic molecular layers that could serve as charge conduits across the entire sample.

We can go further and identify explicitly the *submolecular* channels through which charge flows using the analysis of Figure 2. The DHα6T structure proposed by Garnier et al.[14] can be used after modification in the manner of α6T, where it was found[22,23] that the molecules are inclined to all axes of the unit cell. In fact, electron diffraction (Figure 2a) with the beam normal to the dendritic lamellar crystals which we grew from 0.01% solution in mesitylene (Figure 2b) yields single-crystal patterns (Figure 2c) that correspond closely to those we obtained earlier in single crystals of α6T (cf. Figure 3 in ref 17). Thus the lateral packing of the molecules is expected to be the same in both compounds, the difference lying in the increased length of the *a*-axis[23] due to the presence of the dihexyl end groups. Using this information, we calculate the projected electron potential of DHα6T along the *b*-direction[24] as in Figure 2d, which depicts the contents of a single unit cell with the *a*-axis vertical and the *c*-axis horizontal. The hexathiophene segments of the molecules are seen in the upper and lower thirds of the cell inclined slightly to the *a*-axis, while the hexyl end groups meet in the middle, top, and bottom of the cell. Figure 2e then shows the corresponding calculated high-resolution image from the projected unit cell at the optimal Scherzer defocus of −50.9 nm under the experimental conditions used. Finally, at the underfocus $d^2/2\lambda$ that has been found to maximize the phase contrast of a crystalline lattice of spacing d,[20,25] the resulting calculated image (Figure 2f) demonstrates that the dark fringes are associated with the hexathiophene cores of the molecules and the light regions with the insulating hydrocarbon tails.

On the basis of the above analysis, we show in Figure 3 molecular models of the crystalline lattice of DHα6T

(19) Liao, J.; Martin, D. C. *Science* **1993**, *260*, 1489.
(20) Ojeda, J. R.; Martin, D. C. *Macromolecules* **1993**, *26*, 6557.
(21) Voigt-Martin, I. G.; Simon, P.; Bauer, S.; Ringsdorf, H. *Macromolecules* **1995**, *28*, 236.
(22) Porzio, W.; Destri, S.; Mascherpa, M.; Bruckner, S. *Acta Polym.* **1993**, *44*, 266.
(23) Horowitz, G.; Bachet, B.; Yassar, A.; Lang, P.; Demanze, F.; Fave, J.-L.; Garnier, F. *Chem. Mater.* **1995**, *7*, 1337.
(24) Cerius molecular-modeling package, Molecular Simulations, Inc.
(25) Pradere, P.; Thomas, E. L. *Macromolecules* **1990**, *23*, 4954.

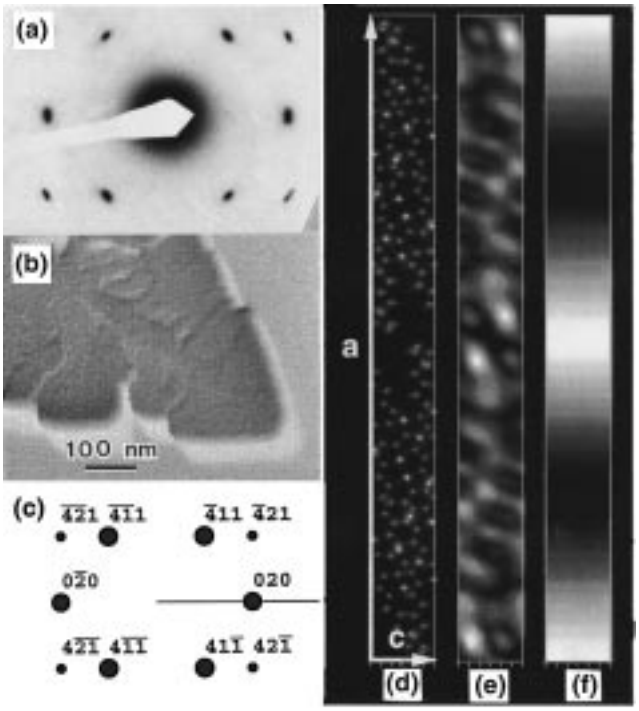

Figure 2. (a) Electron-diffraction pattern from dendritic single crystals of DHα6T grown from dilute solution in mesitylene. (b) The crystal morphology; the preferred growth direction corresponds to the *b*-axis of the unit cell. (c) The calculated electron-diffraction pattern for chains normal to the lamellar crystals, based on the α6T unit cell expanded along the *a*-axis to accommodate the hexyl chains, is in good agreement with the experimental one in panel a. (d) The projected electron potential calculated along the *b*-axis of the unit cell shows that the hydrocarbon tails of the molecules are concentrated at the $a = 0$, $^1/_2$, and 1 positions. The rectangular image corresponds to a single unit cell with the *a*-axis vertical and the *c*-axis horizontal. (e) Simulated image at optimal Scherzer underfocus. (f) Simulated image at optimal $d^2/2\lambda$ underfocus for maximization of the phase contrast of this lattice (d is the lattice spacing and λ the electron wavelength). The white fringes are seen to be associated with the hydrocarbon tails and the black fringes with the hexathiophene cores of the molecules.

and their sub- and supramolecular correspondence to the dark and light electron-microscopic morphological features. In their crystallographic molecular arrangement the dihexyl end groups effectively act as insulating barriers, separating linear assemblies of the hexathiophene cores from each other. As such, they confine the charge carriers within supramolecular pathways of *submolecular* width through which they must travel. That conduction occurs within the hexathiophene cores with no substantial hopping across the hydrocarbon tails is also supported by our studies on dioctadecyl-terminated α6T,[15] as well as by the very large anisotropy in conductivity (ca. 100 times) found for layered DHα6T[14] and for crystals of other thiophene oligomers.[26] Another important aspect of these submolecular pathways is that although the imaged molecules are parallel to the substrate rather than perpendicular, their direction of orbital overlap is still parallel to the substrate, thus preserving the optimal orientation determined for organic thin-film transistor devices. This has also been found to be the preferred orientation for the regioregular polymeric semiconductor poly(3-hexyl thiophene), which is the material from which high-mobility organic TFTs have recently been achieved by printing and stamping technologies.[12]

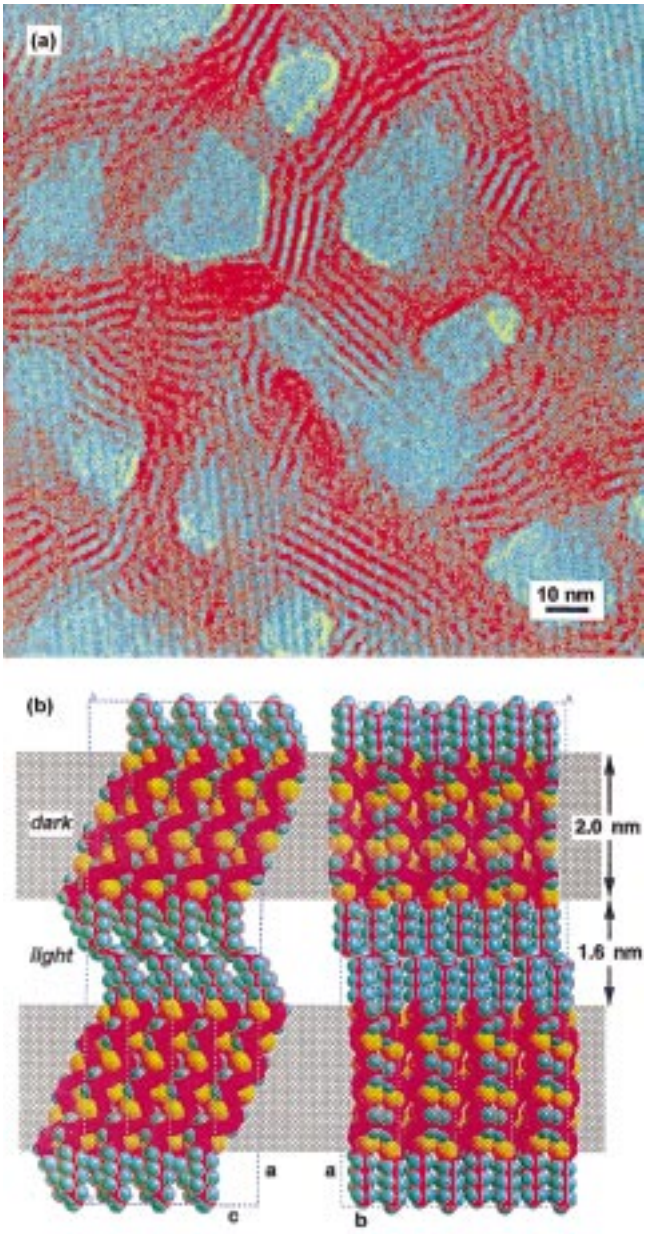

Figure 3. (a) Supramolecular conductive pathways (artificially colored red) in the transmission electron micrographs of DHα6T and (b) their underlying *submolecular* composition as revealed by the packing of DHα6T chains. The dihexyl end groups effectively act as insulating barriers separating stacked assemblies of the hexathiophene core segments from each other. Charges are thus confined to flow within channels of submolecular width consisting of these hexathiophene cores. Color coding is C (red), S (orange), and H (cyan).

(26) Hotta, S.; Waragai, K. *J. Mater. Chem.* **1991**, *1*, 835.

CM980402U